Letter

Development of Cell-Based Sentinels for Nitric Oxide: Ensuring Marker Expression and Unimodality

Ryan McKay, Pricila Hauk, David Quan, and William E Bentley

ACS Synth. Biol., **Just Accepted Manuscript** • DOI: 10.1021/acssynbio.8b00146 • Publication Date (Web): 05 Jul 2018

Development of Cell-Based Sentinels for Nitric Oxide: Ensuring Marker Expression and Unimodality

Ryan McKay,[1,2] Pricila Hauk,[1,2] David Quan,[1,2] and William E. Bentley[1,2]

1. Fischell Department of Bioengineering, University of Maryland, College Park, Maryland

2. Institute for Bioscience and Biotechnology Research, University of Maryland, College Park, Maryland, 20742; telephone: 301-405-4321; fax: 301-405-9953; e-mail: bentley@umd.edu

Abstract

We generated 'sentinel' bacteria that respond to the biomarker, nitric oxide (NO), and produce a homogenous and strong fluorescent response. Our dual-plasmid system consists of a signal 'relay' vector that employs an NO-responsive promoter that amplifies the native signal (via expression of T7 Polymerase (T7Pol)) to a second vector responsible for GFP expression. Importantly, to achieve an optimal 'sentinel' response, we developed strategies that balance the transcriptional load within cells by altering (i) translation and (ii) activity of the T7Pol. Our optimized genetic circuitry was then used to transform commensal *E. coli* Nissle, as a proof-of-concept towards an ingestible cell-based sensor for Crohn's disease (CD) that, in turn, is marked by elevated levels of intestinal NO. Thus, the 'biosensors' demonstrated here may serve as a simple diagnostic tool, contrasting the standard of care including colonoscopies or biopsies.

Keywords: biosensor, probiotics, synthetic biology, signal amplification, inflammatory bowel disease

Biomarkers have for decades been regarded as indicators of disease and organismal health.[1] Cells and materials can be engineered to interact with biomarkers to confer biomarker-induced functionality (e.g. diagnosis or therapeutic intervention). In this work, we engineered a commensal gastrointestinal (GI) bacterium, *E. coli* Nissle 1917, as an indicator of GI dysfunction via the recognition of a GI biomarker, nitric oxide (NO). While engineering promoter regulatory circuits for the expression of easily monitored marker proteins is not new,[2–6] our engineered vector/host system recognizes that heterogeneous responses to chemical cues can be manifest in biased and often misinterpreted results.[7] That is, bacterial cell populations respond both by amplifying gene expression in individual cells and by amplifying the fraction of cells within a population that express the observable and orthogonal marker.[8,9] We have previously shown that engineering the signal-responsive regulatory circuits can yield more homogeneous responses.[10] In the current work, we demonstrate that by partitioning the response into a tailored relay and amplification system, the overall outcome can consist of homogeneous, highly expressing reporter or "sentinel" strains. These, in turn, can be used to indicate the presence of disease or other biomarkers.

The biomarker of this study is nitric oxide (NO), a chemical messenger observed in the pathogenesis of inflammatory or cancerous disease.[11,12] In intestinal fluids of patients with Inflammatory Bowel Disease (IBD), NO is found in concentrations up to 100-fold higher than in healthy individuals.[13,14] Current diagnostic methods rely on invasive colonoscopies and the analysis of biomarkers in stool samples, which are seldom sufficient for an accurate diagnosis.[15–18] Further, there are no practical methods for interrogating intestinal NO. We believe the addition

of facile NO sensing will aid in the diagnosis of IBD and that engineered probiotics may eventually be deployed to both diagnose and treat the disease.

We chose a commensal strain of *E. coli* that responds to nitric oxide, via the *ytfE* and *hmp* promoters, which natively induce protective proteins that quench NO to minimize damage.[19–23] These promoters are repressed by NsrR, and then de-repressed given sufficient intracellular NO.[21] Using these promoters, we engineered bacteria to produce green fluorescent protein (eGFP) in response to NO as a sensing modality, harnessing the *T7* promoter for an amplified response. That is, the *T7* promoter is very strong and often places a notable metabolic burden on the cells.[24] The cumulative effect of plasmid DNA and subsequent T7-amplified expression can result in slowed or suspended growth, as well as mutations that attenuate or abolish protein translation.[25–27] A modified *T7lac* promoter that attenuates such stress was used as a basis in this study.[28] We further altered the distance between the ribosomal binding site (RBS) and the start of the *T7Pol* gene to modulate its translation.[29] In addition, in a combinatorial fashion, we co-expressed the T7 lysozyme (*lysY*) which inhibits T7Pol to modulate *T7lac* promoter activity.[30,31] The subsequent 10 host/vector variants illustrate that the combination of these molecular tools function as fine tuning control "knobs" that provide optimal output of a population of sensor cells.[32,33]

In Figure 1a, wild-type cells transformed with an NO-responsive plasmid express *egfp* via either the *hmp* or *ytfE* promoter. In Fig. 1b, RM02 cells (*E. coli* MG1655 Δ*hmp* with plasmid pRM01) are observed to respond most strongly to NO, perhaps due to their inability to convert NO to nitrate that would otherwise be mediated by Hmp. By comparison, expression from the *ytfE*

promoter increased barely two-fold upon NO addition in the *hmp* mutant. Our findings corroborate those found in literature, where the *hmp* promoter is slightly stronger than *ytfE*, and Δ*hmp* cells are more sensitive due to prolonged exposure to NO.[20–22,34] In the interest of tuning marker expression, we elected to use the stronger *hmp* promoter for all subsequent studies.

In Figure 1, we used diazeniumdiolates (NONOates) for the delivery of bioactive NO. We investigated two popular NONOates, Spermine NONOate (Sper/NO) and DPTA NONOate (DPTA/NO) as NO-releasing compounds for characterizing cell genetic and phenotypic responses (see Supplemental).[20,21,34] In Figure S1a for both RM01 and RM02 cells, Sper/NO treatment resulted in a dose-dependent response. In the case of DPTA/NO, Δ*hmp* host cells (RM02) produced more eGFP at 50μM than at all other concentrations as well as at all conditions in WT (RM01) cells. We note however, that the eGFP produced by RM02 cells was reduced at increased NO beyond 50μM. Also, the growth rate of cells was reduced upon exposure to higher levels of DPTA/NO and in an apparent dose dependent manner (Figure S1c). We suspected this was due to the lack of a genomic NO-dissimilation response and decided to use WT hosts for the remainder of our studies. Importantly, the NO levels tested here mimic physiological NO levels in IBD (micromolar range),[11,35] as 50μM NONOates (~1μM NO consistently released over the timecourse)[34,36] were used for the remaining studies, owing to the high levels of gene expression and relatively minimal effects on cell growth.

While the above cells fluoresced in the presence of NO, we found the level of eGFP expression was low (Figure S2.). We then implemented a T7Pol amplification strategy,[37] employing the native *hmp* promoter to express *T7Pol* from a 'relay' plasmid in WT cells and coupled this with a

T7lac promoter to drive eGFP on a second reporter plasmid. Our initial attempts, however, using RM40 cells (WT + pRM44/pRM100) resulted in no fluorescence upon NO exposure. Owing to our previous findings,[37] we hypothesized that the amplification circuit imposed too much of a metabolic drain on the cells. Hence, we attenuated the *T7lac* activity while retaining the native *hmp* promoter activity as the original signal cue: (i) we decreased translation rate of T7Pol and/or (ii) increased the inhibition of T7Pol via expression of T7 lysozyme, as illustrated in Figure 1c. Specifically, a library of 10 host/vector strains was created in which the sensor plasmids encode T7Pol alone (pRM4X) or concomitantly with LysY (pRM5X, Fig 1c), and "X" denotes the inclusion of 0, 3, 6, 9, and 12 additional nonsense spacer nucleotides (for X = 0,1,2,3,4, respectively) inserted between the putative RBS and structural gene.

The variants' capabilities to produce eGFP in response to NO are demonstrated in Figure 2. In all cases we used fluorescence activated cell sorting (FACS) to quantify output. This enables discrimination of the per cell fluorescence as well as the uniformity in the response among the entire sensing population. In Fig. 2a, FACS data are presented with windows demarcating the population of cells fluorescing green. In Fig. 2b, the coefficient of variance (CV) of the population's fluorescence intensity indicates the uniformity of response, and this is plotted against the fraction of the total population that expresses eGFP. Thus, populations with a low CV and high percentage of fluorescent cells respond most uniformly. The magnitude of fluorescence intensity for these cells is illustrated in Fig. 2a., along the x-axis.

In cells without the T7 lysozyme (RM4X), only RM43 and RM44 cells, the variants with the longest RBS-*T7Pol* spacing, produced a significant fluorescence response. Interestingly, we

found that RM44 exhibited a continuous and somewhat broadly distributed response, while RM43 cells exhibited a bimodal population distribution with roughly half the cells fluorescing brighter than RM44, and half not fluorescing. We note also that a sizable number of RM43 cells in the negative control cultures (0μM NO) were fluorescent (Figure S3), suggesting a metabolically stable level of leaky expression of *T7Pol*, but an intolerable 'burden' when induced. That is, we suspected a sub-population of cells was presumably experiencing excessive *T7lac* regulated transcription precluding GFP expression. Parenthetically, we noticed an elongated morphology (Fig. S4), which has been suggested an outcome of excessive *T7lac* activity.[31] Given only a small amount of T7Pol is needed to induce the *T7lac* promoter, we believe the leaky expression of *T7Pol* in RM40-42 cells caused an excessive transcriptional burden resulting in no eGFP in either induced or uninduced cells (Figs. 2, S3, and S5).

Similarly, Figure 2 also shows variants (RM5X) with altered RBS-*T7Pol* spacing. Here, all cells constitutively expressed a low but constant level of the T7 lysozyme, *lysY* (pRM5X plasmids have the low copy origin of replication, pSC101). A readily observed difference when compared to their RM4x counterparts, was that cells with little or no additional RBS-*T7Pol* spacing (RM40-42 vs. RM50-52) were able to produce high levels of eGFP. Images of all samples are provided in Figure S5. Interestingly, we found that about half of the RM50 population was fluorescent, similar to RM43 cells. As depicted in Fig 2e, we hypothesized that the similarity between RM50 and RM43 was due to these cells having similar levels of T7Pol. In support of this hypothesis, when we decreased T7Pol levels via additional RBS-*T7Pol* spacing, we found that RM51 and RM52 cells were more fluorescent than RM50 in terms of the fraction of fluorescing cells. Both RM51 and RM52 cells were highly and uniformly fluorescent when

induced, although RM51 cells had more leaky expression (Fig. S3), making RM52 cells a better candidate for a switch-like sensor. The addition of more nucleotides (nt's) prior to *T7Pol* (in RM53 and RM54 cells) lowered and ultimately abolished *egfp* expression. When considering the differences between the RM44 and RM54 populations, RM54 had both the largest number of inserted nucleotides with co-expression of LysY, representing the case with most severe attenuation of eGFP expression. That a more diverse response was observed in RM44 cells, suggests that (i) there was more than an adequate number of T7 lysozyme to inhibit the T7Pol levels in RM54, and (ii) that the heterogeneity in RM44 response was not due to the cell's access to the NO, but rather the heterogeneity in the *hmp* promoter response within the cells.

We considered these attributes when constructing the ideal "sentinel" biosensing cells. An ideal response would be as binary as possible: uninduced cells should be "off" and induced uniformly "on". To that end, the pRM44 and pRM52 plasmid systems were best suited based on their unimodal/homogenous population responses. We note that due to the small changes in speculated T7Pol levels that lead to large population shifts (unimodal vs. bimodal), the average fluorescence of an entire population should be used with caution when assessing an eGFP response (see Fig. S3b).

The best variants from Fig. 2a were further characterized by interrogating how quickly eGFP was produced in the presence of NO, as well as the sensitivity of these cells to various levels of NONOate. Figure 2c revealed that the response in RM52 cells was quicker and expectedly stronger than RM44; after 90 minutes the fluorescence of RM52 cells was ~8-fold greater. Importantly, both RM44 and RM52 exhibited a minimal response to low levels of NO, yet after a

threshold of ~1μM NONOate were found to significantly express *egfp* (Fig. 2d). Further, in RM52 cells with just 5μM, the response peaked and plateaued, while RM44 cells required nearly a 20-fold greater NONOate dosage to reach its full response level. Analogously developed NO-sensing cells that did not feature the T7 amplification system, but instead relied on a native promoter (*norV*), only reached a homogeneous response after ~100 μM NONOate.[2] Applying logistic equations to the data in Fig. 2d reveals that in addition to lower fluorescent levels, RM44 cells are less suitable as a switch-like visual sensor due to the poor fit and lack of an apparent step increase in fluorescence. Conversely, the agreement between the data and the curve for RM52 cells, coupled with the high magnitude of fluorescent output, indicates an ideal response mechanism for a switch-like biosensor, whereby low basal levels of NO (nanomolar or below) should not elicit a fluorescent output, while elevated levels may induce a saturated response.

Cumulatively, these observations were used to generate the illustration in Figure 2e, which suggests a correlation between the fluorescent output (green band intensity) to a hypothesized level of "free T7Pol". The two lines depicted show the strains with and without *lysY* expression. That is, all RM5X plasmids have T7 lysozyme that putatively sequesters T7Pol rendering it inactive.[30,31] This line is depicted roughly parallel to the line of the RM4X cells. Here, the attenuation of T7Pol translation is the only effector and is due to the RBS-ATG spacing. Thus, we suspect that in the cases of RM40-42, the sensor and relay plasmid system creates too much of a load on the cells precluding expression of eGFP (hence these points are above the green band). As the sequestration of T7Pol via LysY is difficult to assess, these concepts are as yet unproven. Nonetheless, the apparent influence of T7 lysozyme is clear in that it titrates T7Pol activity, which in turn is heterogeneous in the current system.

For a bacterial biosensor to be deployed in humans, a safe and approved probiotic host is important. Thus, we next transformed these vectors into the commensal *E. coli* Nissle 1917 (EcN) host exactly analogously to W3110 RM44 and RM52 to generate RM90 and RM91, respectively. As anticipated, the plasmids conferred similar results. Figure 3a presents flow cytometry data for the engineered Nissle biosensors. The RM91 cells exhibited a strong unimodal response and the RM90 cells exhibited a unimodal response that was more broadly distributed and slightly attenuated in comparison. It is important to underscore that the genetic sensor system comprising two plasmids, the first exploiting the native response element and the amplification modality and the second providing the marker protein, was fully transportable to a completely different host.

Subsequently, we utilized an *in vitro* model for assessing a response to NO released from epithelial cells (Fig. 3b). Briefly, confluent Caco-2 cells were grown in DMEM medium on a transwell insert to simulate the intestinal epithelium. We exposed a sub-group of cells to the inflammatory cytokine IFN-γ and agonist PMA, to induce NO production, mimicking inflammation. We then introduced RM90 and RM91 cells to the top of the device (i.e. the "lumen" of the Caco-2 monolayer) for 90 minutes. Following this co-culture, bacteria were removed and analyzed via flow cytometry. Figures 3c and S10 reveal that the engineered probiotic exposed to inflamed Caco-2 cells exhibited increased fluorescence (~2-fold increase in both mean and percent fluorescent cells).

In summary, the dual-plasmid circuit designed here to amplify a bacterial response to nitric oxide

was used to develop a homogenous and switch-like response to NO elicited from epithelial cells. These 'sentinel' cells could next be used as a natural sensing population for interrogating the GI tract, as explored by Archer et al.[2] Briefly, their use as a diagnostic tool may be accomplished via ingestion of engineered cells within a capsule, followed by analysis of cells extracted from a stool sample with fluorescent microscopy.[38] Engineered cells are then intended to provide non-invasive assessment preceding further diagnostic processes such as biopsies, or perhaps as replacements of current invasive procedures. That is, investigations of engineered commensal bacteria for the purpose of monitoring and potentially modulating health have appeared and show promise.[39–42] Hwang et al. (2017) relied on gavage addition of 'smart' bacteria to mice instead of a capsule. In their application, the engineered bacteria recognized disease-specific signal molecules and then expressed and secreted a therapeutic.[40] Thompson et al. (2015) showed how engineered bacteria can be used to intentionally alter the balance of the microbiome.[43] Certainly, delivery issues and others such as horizontal gene transfer, bacterial fate, and control are being evaluated in these studies. In our case, we could swap *egfp* for the gene(s) of a biotherapeutic that is produced in response to localized release of NO, enabling the probiotic cells to overproduce therapeutic proteins in the presence of inflammation. Similarly, exchanging the promoter may facilitate sensing of other biomolecules for other applications, using the platform presented here to achieve a uniform response.

Materials and Methods

Strains and Growth Conditions. K-12 W3110 or MG1655, or Nissle 1917 *E. coli* were used. Cells were grown overnight and re-inoculated the following day in LB media supplemented with antibiotics at 50μg/ml. Cells were spun down near an OD_{600} of 0.2 and resuspended in M9

minimal media supplemented with glucose (0.4% w/v), vitamin B1 (1mM) and Casamino acids (0.5g/L) with antibiotics to OD_{600} ~ 0.2. Cells were induced with Spermine/NONOate or DPTA/NONOate (Cayman Chemical) at 50μM, unless otherwise specified. Genomic deletion of *hmp* in *E. coli* K-12 W3110 was carried out using the method described by Datsenko and Wanner.[44] Other than during the *hmp* deletion, which requires 30°C, cells were grown at 37°C, shaking at 250rpm. A list of strains is found in Table 1. A list of plasmids and their construction methods are detailed in Supplemental Information.

Flow cytometry. Flow cytometry samples were recorded as-is (i.e. in M9 or LB media) using a BD FACSCantoII (Becton Dickson) analyzer with FACSDiva software. Phosphate buffered saline (PBS) was used to dilute samples to ensure a regulated event abort rate (100 per second or less). Sample sizes of 50,000 cells within a gate determined by forward and side scatter voltages of 525 and 425, respectively, were recorded unless otherwise specified. Either 650V or 400V were used for the FITC (green) fluorescent analyses. For time-course experiments, 200μL of sample was pelleted and resuspended in an equal volume of 2% paraformaldehyde in PBS. Data presented are from a single experiment, representative of biological replicates run on different days, except samples derived from the inflamed mammalian cell investigation were from a single day using biological duplicates.

Fluorescence Microscopy. Cells were imaged using CellSens software (Olympus) and a DX60 microscope equipped with a DP72 camera (Olympus), using a 20x objective lens with 500ms exposure time.

Mammalian Cell Culture and Inflammation Model. Rat collagen type I (Corning) was used to coat overnight 24-well transwell inserts (Corning) at a concentration of 10μg/cm^2, as per the

manufacturers protocol. Caco-2 cells (ATCC) were seeded at $3x10^5$ cells/cm^2 on the coated transwell inserts, and cultured in DMEM with 20mM HEPES, 1% non-essential amino acids, 1% Pen-strep, 4.5g/L D-glucose, 4mM L-glutamine, 110mg/L sodium pyruvate with 10% fetal bovine serum at 37°C with 5% CO_2. Media changes occurred every 2-3 days, and cells were maintained for 24 days to ensure post-confluent differentiation. Transepithelial electric resistance (TEER) was measured weekly to verify confluence. On day 24, media without antibiotics but including 200nM phorbol 12-myristate 13-acetate (PMA) and 10,000U/mL interferon-gamma (IFN-γ) was added to the basolateral side of the cells, similar to previous studies.[45,46] Media without antibiotics was added to the apical side, and incubated for 24 hours. Then, ~$3x10^7$ log-phase bacteria in PBS were added to the apical side, and incubated for 90 minutes. The apical volume was then removed and bacteria were analyzed via flow cytometry.

Acknowledgements. Dr. Mark Brynildsen, Dr. Jonathan Robinson, Dr. Stephen Spiro, and Dr. Rodolfo Urbano answered questions to assist in this study. MG1655 Δ*hmp* cells were a gift from Dr. Mark Brynildsen (Princeton). The plasmid pBbS8a was a gift from Dr. Matthew Wook Chang (Singapore). This work was supported by DTRA (HDTRA1-13-0037), NSF (CBET #1160005), and USDA (NIFA #2014-67021-21585).

Author Contributions. R.M. provided concept design and conducted all experiments, analyzed data, and wrote the manuscript. P.H. provided extensive guidance on cloning and molecular biology concepts. D.Q. assisted with the mammalian cell experiments. W.B. provided guidance and assisted with manuscript preparation.

Supporting Information. A PDF file containing supplemental methods, tables of plasmids relevant to the study, figures to accompany the main body text, and subsequent discussion of these figures as needed.

References

(1) Strimbu, K., and Tavel, J. a. (2011) What are Biomarkers? *Curr Opin HIV AIDS 5*, 463–466.
(2) Archer, E. J., Robinson, A. B., and Süel, G. M. (2012) Engineered E. coli that detect and respond to gut inflammation through nitric oxide sensing. *ACS Synth. Biol. 1*, 451–7.
(3) Lu, C., Albano, C. R., Bentley, W. E., and Rao, G. (2005) Quantitative and kinetic study of oxidative stress regulons using green fluorescent protein. *Biotechnol. Bioeng. 89*, 574–587.
(4) Kotula, J. W., Kerns, S. J., Shaket, L. A., Siraj, L., Collins, J. J., Way, J. C., and Silver, P. A. (2014) Programmable bacteria detect and record an environmental signal in the mammalian gut. *Proc. Natl. Acad. Sci. 111*, 4838–4843.
(5) Riglar, D. T., Giessen, T. W., Baym, M., Kerns, S. J., Niederhuber, M. J., Bronson, R. T., Kotula, J. W., Gerber, G. K., Way, J. C., and Silver, P. A. (2017) Engineered bacteria can function in the mammalian gut long-term as live diagnostics of inflammation. *Nat. Biotechnol. 35*, 653–658.
(6) Daeffler, K. N., Galley, J. D., Sheth, R. U., Ortiz-Velez, L. C., Bibb, C. O., Shroyer, N. F., Britton, R. A., and Tabor, J. J. (2017) Engineering bacterial thiosulfate and tetrathionate sensors for detecting gut inflammation. *Mol. Syst. Biol. 13*, 923.
(7) Garcia, J. R., Cha, H. J., Rao, G., Marten, M. R., and Bentley, W. E. (2009) Microbial nar-GFP cell sensors reveal oxygen limitations in highly agitated and aerated laboratory-scale fermentors. *Microb. Cell Fact. 8*, 1–7.
(8) Servinsky, M. D., Terrell, J. L., Tsao, C.-Y., Wu, H.-C., Quan, D. N., Zargar, A., Allen, P. C., Byrd, C. M., Sund, C. J., and Bentley, W. E. (2016) Directed assembly of a bacterial quorum. *ISME J. 10*, 158–169.
(9) Siegele, D. A., and Hu, J. C. (1997) Gene expression from plasmids containing the araBAD promoter at subsaturating inducer concentrations represents mixed populations. *Proc. Natl. Acad. Sci. U. S. A. 94*, 8168–8172.
(10) Zargar, A., Quan, D. N., and Bentley, W. E. (2016) Enhancing Intercellular Coordination: Rewiring Quorum Sensing Networks for Increased Protein Expression through Autonomous Induction. *ACS Synth. Biol. 5*, 923–928.
(11) Stanek, A., Gadowska-Cica, A., Gawron, K., Wielkoszynski, T., Adamek, B., Cieslar, G., Wiczkowski, A., and Sieron, A. (2008) Role of nitric oxide in the gastrointestinal tract. *Mini-Reviews Med. Chem. 8*, 2–7.
(12) Shah, V., Lyford, G., Gores, G., and Farrugia, G. (2004) Nitric Oxide in Gastrointestinal Health and Disease. *Gastroenterology 126*, 903–913.
(13) Reinders, C. I., Herulf, M., Ljung, T., Hollenberg, J., Weitzberg, E., Lundberg, J. O., and Hellström, P. M. (2005) Rectal mucosal nitric oxide in differentiation of inflammatory bowel

disease and irritable bowel syndrome. *Clin. Gastroenterol. Hepatol. 3*, 777–783.
(14) Lundberg, J. O. N., Hellström, P. M., Lundberg, J. M., and Alving, K. (1994) Greatly increased luminal nitric oxide in ulcerative colitis. *Lancet 344*, 1673–1674.
(15) Langhorst, J., Elsenbruch, S., Koelzer, J., Rueffer, A., Michalsen, A., and Dobos, G. J. (2008) Noninvasive Markers in the Assessment of Intestinal Inflammation in Inflammatory Bowel Diseases: Performance of Fecal Lactoferrin, Calprotectin, and PMN-Elastase, CRP, and Clinical Indices. *Am. J. Gastroenterol. 103*, 162–169.
(16) Lewis, J. D. (2011) The Utility of Biomarkers in the Diagnosis and Therapy of Inflammatory Bowel Disease. *Gastroenterology 140*, 1817–1826.
(17) von Roon, A. C., Karamountzos, L., Purkayastha, S., Reese, G. E., Darzi, A. W., Teare, J. P., Paraskeva, P., and Tekkis, P. P. (2007) Diagnostic Precision of Fecal Calprotectin for Inflammatory Bowel Disease and Colorectal Malignancy. *Am. J. Gastroenterol. 102*, 803–813.
(18) Lasson, A., Kilander, A., and P., S. (2008) Diagnostic yield of colonoscopy based on symptoms. *Scand J Gastroenterol. 43*, 356–362.
(19) Vasudevan, S. G., Armarego, W. L. F., Shawl, D. C., Lilley, P. E., Dixon, N. E., and Poole, R. K. (1991) Isolation and nucleotide sequence of the hmp gene that encodes a haemoglobin-like protein in Escherichia coli K-12. *MGG Mol. Gen. Genet. 226*, 49–58.
(20) Filenko, N., Spiro, S., Browning, D. F., Squire, D., Overton, T. W., Cole, J., and Constantinidou, C. (2007) The NsrR regulon of Escherichia coli K-12 includes genes encoding the hybrid cluster protein and the periplasmic, respiratory nitrite reductase. *J. Bacteriol. 189*, 4410–4417.
(21) Bodenmiller, D. M., and Spiro, S. (2006) The yjeB (nsrR) Gene of Escherichia coli Encodes a Nitric Oxide-Sensitive Transcriptional Regulator. *J. Bacteriol. 188*, 874–881.
(22) Robinson, J. L., and Brynildsen, M. P. (2013) A Kinetic Platform to Determine the Fate of Nitric Oxide in Escherichia coli. *PLoS Comput. Biol. 9*, e1003049.
(23) Justino, M. C., Almeida, C. C., Teixeira, M., and Saraiva, L. M. (2007) Escherichia coli Di-iron YtfE protein is necessary for the repair of stress-damaged iron-sulfur clusters. *J. Biol. Chem. 282*, 10352–10359.
(24) Studier, F. W., and Moffatt, B. A. (1986) Use of bacteriophage T7 RNA polymerase to direct selective high-level expression of cloned genes. *J. Mol. Biol. 189*, 113–130.
(25) Kurland, C. G., and Dong, H. (1996) Bacterial growth inhibition by overproduction of protein. *Mol. Microbiol. 21*, 1–4.
(26) Dong, H., Nilsson, L., Kurland, C. G., Dong, H., Nilsson, L., and Kurland, C. G. (1995) Gratuitous overexpression of genes in Escherichia coli leads to growth inhibition and ribosome destruction. *J. Bacteriol. 177*, 1497–1504.
(27) Bentley, W. E., Mirjalili, N., Andersen, D. C., Davis, R. H., and Kompala, D. S. (1990) Plasmid-encoded protein: The principal factor in the “metabolic burden” associated with recombinant bacteria. *Biotechnol. Bioeng. 35*, 668–681.
(28) Alexander, W. A., Moss, B., and Fuerst, T. R. (1992) Regulated expression of foreign genes in vaccinia virus under the control of bacteriophage T7 RNA polymerase and the Escherichia coli lac repressor. *J. Virol. 66*, 2934–42.
(29) Chen, H., Bjerknes, M., Kumar, R., and Jay, E. (1994) Determination of the optimal aligned spacing between the Shine-Dalgarno sequence and the translation initiation codon of *E. coli* mRNAs. *Nucleic Acids Res. 22*, 4953–4957.
(30) Moffatt, B. A., and Studier, F. W. (1987) T7 lysozyme inhibits transcription by T7 RNA polymerase. *Cell 49*, 221–227.

(31) Studier, F. W. (1991) Use of bacteriophage T7 lysozyme to improve an inducible T7 expression system. *J. Mol. Biol. 219*, 37–44.
(32) Soriano, E., Borth, N., Katinger, H., and Mattanovich, D. (2002) Optimization of recombinant protein expression level in Escherichia coli by flow cytometry and cell sorting. *Biotechnol. Bioeng. 80*, 93–99.
(33) Wagner, S., Klepsch, M. M., Schlegel, S., Appel, A., Draheim, R., Tarry, M., Wijk, K. J. Van, Slotboom, D. J., Persson, J. O., and de Gier, J.-W. (2008) Tuning Escherichia coli for membrane protein overexpression *105*, 14371–14376.
(34) Robinson, J., and Brynildsen, M. (2016) Construction and Experimental Validation of a Quantitative Kinetic Model of Nitric Oxide Stress in Enterohemorrhagic Escherichia coli O157:H7. *Bioengineering 3*, 9.
(35) Laurent, M., Lepoivre, M., and Tenu, J. P. (1996) Kinetic modelling of the nitric oxide gradient generated in vitro by adherent cells expressing inducible nitric oxide synthase. *Biochem. J. 314*, 109–113.
(36) Ramamurthi, A., and Lewis, R. S. (1997) Measurement and modeling of nitric oxide release rates for nitric oxide donors. *Chem. Res. Toxicol. 10*, 408–413.
(37) Tsao, C. Y., Hooshangi, S., Wu, H. C., Valdes, J. J., and Bentley, W. E. (2010) Autonomous induction of recombinant proteins by minimally rewiring native quorum sensing regulon of E. coli. *Metab. Eng. 12*, 291–297.
(38) Schultz, M., Watzl, S., Oelschlaeger, T. A., Rath, H. C., Göttl, C., Lehn, N., Schölmerich, J., and Linde, H. J. (2005) Green fluorescent protein for detection of the probiotic microorganism Escherichia coli strain Nissle 1917 (EcN) in vivo. *J. Microbiol. Methods 61*, 389–398.
(39) Hwang, I. Y., Tan, M. H., Koh, E., Ho, C. L., Poh, C. L., and Chang, M. W. (2014) Reprogramming Microbes to be Pathogen-Seeking Killers. *ACS Synth. Biol. 3*, 228–237.
(40) Hwang, I. Y., Koh, E., Wong, A., March, J. C., Bentley, W. E., Lee, Y. S., and Chang, M. W. (2017) Engineered probiotic Escherichia coli can eliminate and prevent Pseudomonas aeruginosa gut infection in animal models. *Nat. Commun. 8*, 15028.
(41) Goh, Y.-L., He, H., and March, J. C. (2012) Engineering commensal bacteria for prophylaxis against infection. *Curr. Opin. Biotechnol. 23*, 924–30.
(42) Wu, H.-C., Tsao, C.-Y., Quan, D. N., Cheng, Y., Servinsky, M. D., Carter, K. K., Jee, K. J., Terrell, J. L., Zargar, A., Rubloff, G. W., Payne, G. F., Valdes, J. J., and Bentley, W. E. (2014) Autonomous bacterial localization and gene expression based on nearby cell receptor density. *Mol. Syst. Biol. 9*, 636–636.
(43) Thompson, J. A., Oliveira, R. A., Djukovic, A., Ubeda, C., and Xavier, K. B. (2015) Manipulation of the quorum sensing signal AI-2 affects the antibiotic-treated gut microbiota. *Cell Rep. 10*, 1861–1871.
(44) Datsenko, K. A., and Wanner, B. L. (2000) One-step inactivation of chromosomal genes in Escherichia coli K-12 using PCR products. *Proc Natl Acad Sci 97*, 6640–5.
(45) Vignoli, A. L., Srivastava, R. C., Stammati, A., Turco, L., Tanori, M., and Zucco, F. (2001) Nitric oxide production in Caco-2 cells exposed to different inducers, inhibitors and natural toxins. *Toxicol. Vitr. 15*, 289–295.
(46) Chen, X.-M., and Kitts, D. D. (2008) Determining conditions for nitric oxide synthesis in Caco-2 cells using Taguchi and factorial experimental designs. *Anal. Biochem. 381*, 185–192.

Table 1. List of strains used

Strain	Characteristics/Genotype	Reference
W3110 (WT)	K-12, F$^-$, λ$^-$, INV(*rrnD*, *rrnE*), *rph*-1	Coli Genetic Stock Center, Yale University (New Haven, CT)
MG1655 (WT)	K-12, F$^-$, λ$^-$, *ilvG*$^-$, *rfb*-50, *rph*-1	Coli Genetic Stock Center, Yale University (New Haven, CT)
Nissle 1917 (Mutaflor)	*E. coli* DSM 6601, serotype O6:K5:H1	Aralez Pharmaceuticals (Mississauga, ON, Canada)
Δ*hmp*	MG1655 Δ*hmp*	Coli Genetic Stock Center, Yale University (New Haven, CT)
RM00	W3110 Δ*hmp*::Cm^r	This study
RM01	MG1655 WT with pRM01	This study
RM02	MG1655 Δ*hmp* with pRM01	This study
RM03	MG1655 WT with pRM02	This study
RM04	MG1655 Δ*hmp* with pRM02	This study
RM05	W3110 WT with pRM01	This study
RM06	W3110 Δ*hmp* with pRM01	This study
RM40	W3110 WT with pRM40 and pRM100	This study
RM41	W3110 WT with pRM41 and pRM100	This study
RM42	W3110 WT with pRM42 and pRM100	This study
RM43	W3110 WT with pRM43 and pRM100	This study
RM44	W3110 WT with pRM44 and pRM100	This study
RM50	W3110 WT with pRM50 and pRM100	This study
RM51	W3110 WT with pRM51 and pRM100	This study
RM52	W3110 WT with pRM52 and pRM100	This study
RM53	W3110 WT with pRM53 and pRM100	This study
RM54	W3110 WT with pRM54 and pRM100	This study
RM90	Nissle 1917 with pRM44 and pRM100	This study
RM91	Nissle 1917 with pRM52 and pRM100	This study

Figure 1. (a) A wild-type cell with a nitric oxide (NO) responsive plasmid. NO de-depresses NsrR from the *hmp* promoter to produce Hmp, which converts harmful NO to nitrate as a means of detoxification. The *hmp* or *ytfE* promoters are regulated by NsrR on a low copy plasmid to produce a gene of interest. **(b)** Representative flow cytometry data of approximately 50,000 cells using a FITC voltage of 650V after 90 minutes of induction with 50μM NONOate. Normalized values indicate that each sample is subtracted by its respective mean fluorescence for an uninduced sample. Error bars are standard error. **(c)** Genetic circuit to amplify gene expression under the *hmp* promoter using a dual-plasmid system. RM5x cells shown alter the RBS-*T7Pol* spacing and produce the T7 lysozyme. **(d)** View of the interface between the RBS and *T7Pol* to show where extra nucleotides are inserted at **X**.

Figure 2. (a) Plots of representative flow cytometry data from RM4x and RM5x cells using a FITC voltage of 400V after 90 min induction with 50μM NONOate. Values in parentheses are mean fluorescence of the gated fluorescent population. **(b)** Coefficient of variance (CV) of the entire cell population is plotted against the mean fluorescence of cells. **(c)** Representative mean fluorescence of RM44 and RM52 cells during 90 minutes of induction with 50uM NONOate. **(d)** Mean fluorescence of the same cells after 90 min, as a function of NONOate concentration. Lines are fit logistic functions of the data. **(e)** Representation of the effects of attenuation of T7Pol translation and/or inclusion of the T7 lysozyme on free T7Pol levels in RM4x and RM5x cells upon induction. Green shading indicates accompanying *T7lac* activity (eGFP production), informed from **(a)**. Error bars represent standard error, and data points are gathered using approximately 50,000 cells.

Figure 3. (a) Representative flow cytometry data of approximately 50,000 Nissle 1917 host cells per plot, using a FITC voltage of 400V after 90 minutes of induction. The gate to determine the fluorescent population is defined as anything above the population of a negative control of non-fluorescent cells. Y-axis is cell count and X-axis is FITC (fluorescence) intensity. **(b)** Schematic of the IBD *in vitro* assay to stimulate engineered bacteria with biologically produced NO. Bacteria are incubated in the apical side of the transwell insert and assessed via FACS. **(c)** The percentage of the total population of cells that are above a threshold fluorescence from the assay illustrated in (b), plot as the average of biological duplicates. Error bars are standard error.

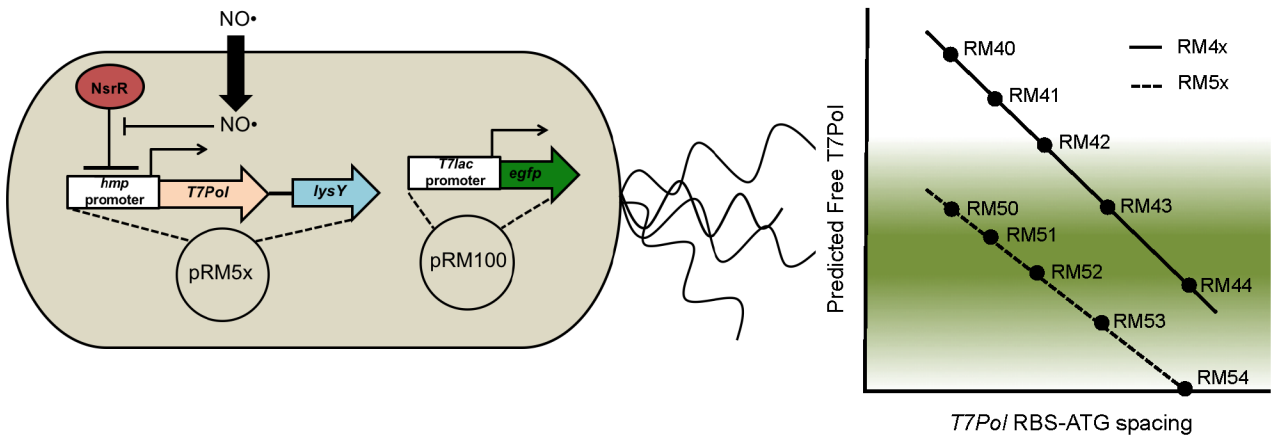
NO•
NsrR
NO•
hmp promoter
T7Pol
lysY
T7lac promoter
egfp
pRM5x
pRM100
Predicted Free T7Pol
RM40
RM41
RM42
RM43
RM44
RM50
RM51
RM52
RM53
RM54
RM4x
RM5x
T7Pol RBS-ATG spacing

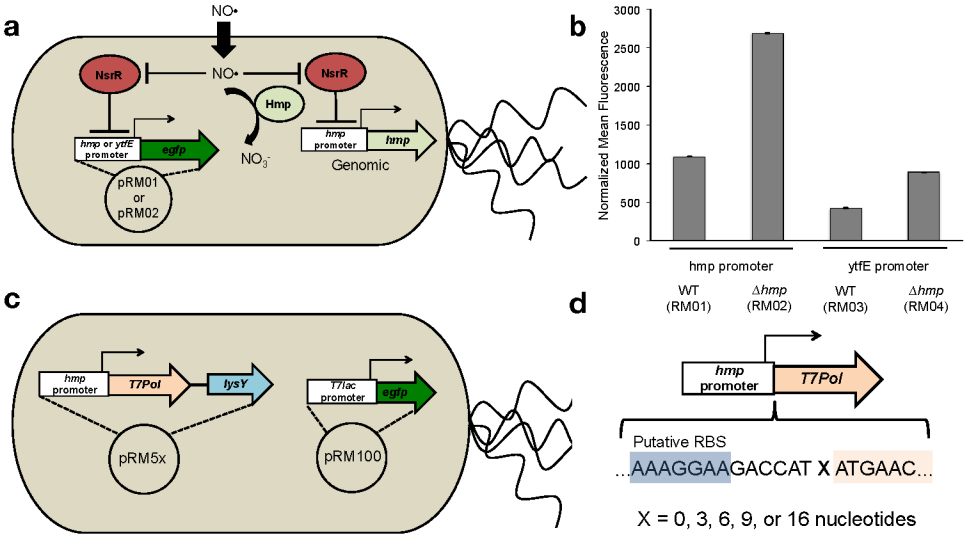

Figure 1. (a) A wild-type cell with a nitric oxide (NO) responsive plasmid. NO de-depresses NsrR from the *hmp* promoter to produce Hmp, which converts harmful NO to nitrate as a means of detoxification. The *hmp* or *ytfE* promoters are regulated by NsrR on a low copy plasmid to produce a gene of interest. **(b)** Representative flow cytometry data of approximately 50,000 cells using a FITC voltage of 650V after 90 minutes of induction with 50μM NONOate. Normalized values indicate that each sample is subtracted by its respective mean fluorescence for an uninduced sample. Error bars are standard error. **(c)** Genetic circuit to amplify gene expression under the *hmp* promoter using a dual-plasmid system. RM5x cells shown alter the RBS-*T7Pol* spacing and produce the T7 lysozyme. **(d)** View of the interface between the RBS and *T7Pol* to show where extra nucleotides are inserted at **X**.

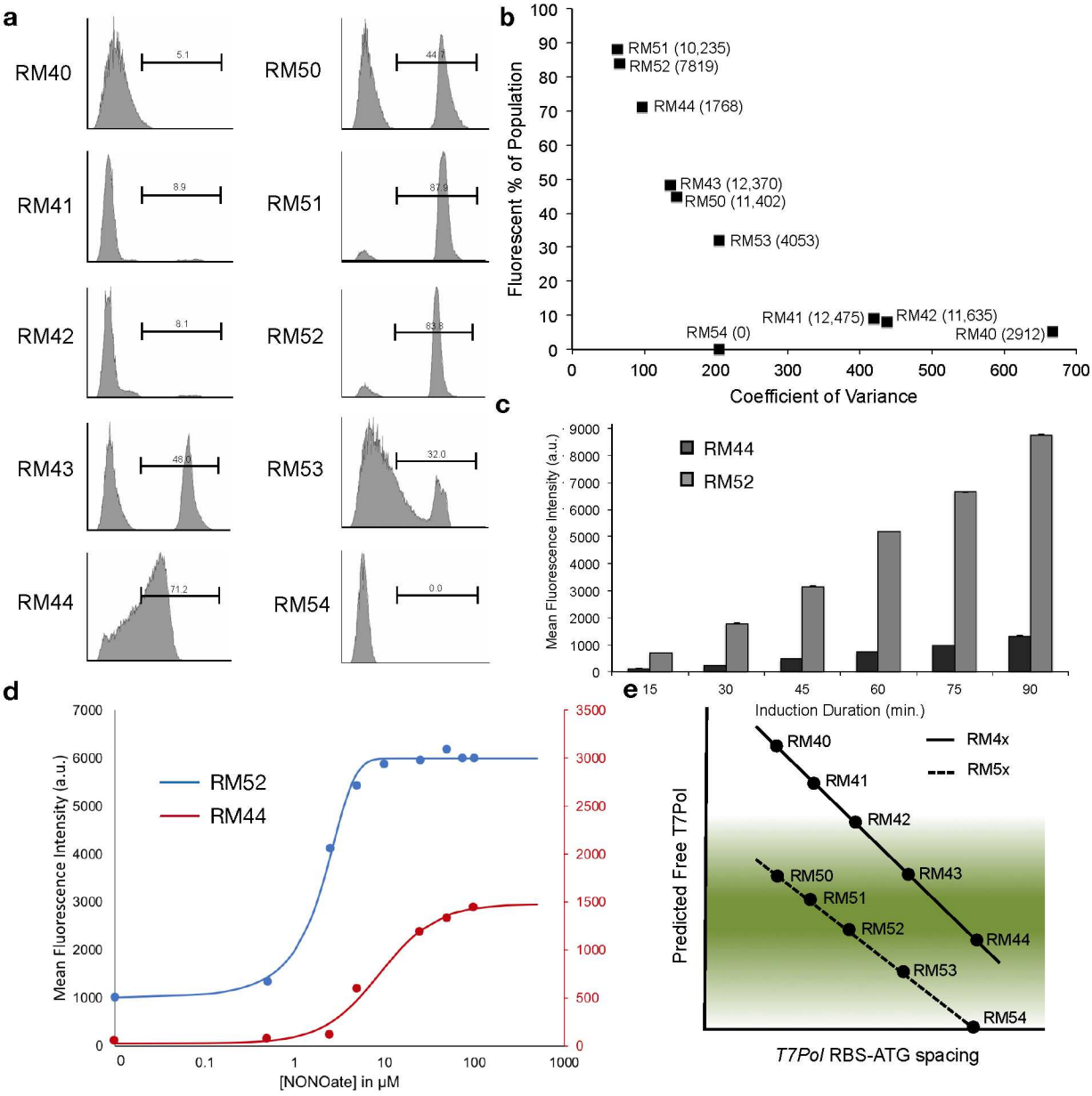

Figure 2. (a) Plots of representative flow cytometry data from RM4x and RM5x cells using a FITC voltage of 400V after 90 min induction with 50μM NONOate. Values in parentheses are mean fluorescence of the gated fluorescent population. **(b)** Coefficient of variance (CV) of the entire cell population is plotted against the mean fluorescence of cells. **(c)** Representative mean fluorescence of RM44 and RM52 cells during 90 minutes of induction with 50uM NONOate. **(d)** Mean fluorescence of the same cells after 90 min, as a function of NONOate concentration. Lines are fit logistic functions of the data. **(e)** Representation of the effects of attenuation of T7Pol translation and/or inclusion of the T7 lysozyme on free T7Pol levels in RM4x and RM5x cells upon induction. Green shading indicates accompanying *T7lac* activity (eGFP production), informed from **(a)**. Error bars represent standard error, and data points are gathered using approximately 50,000 cells.

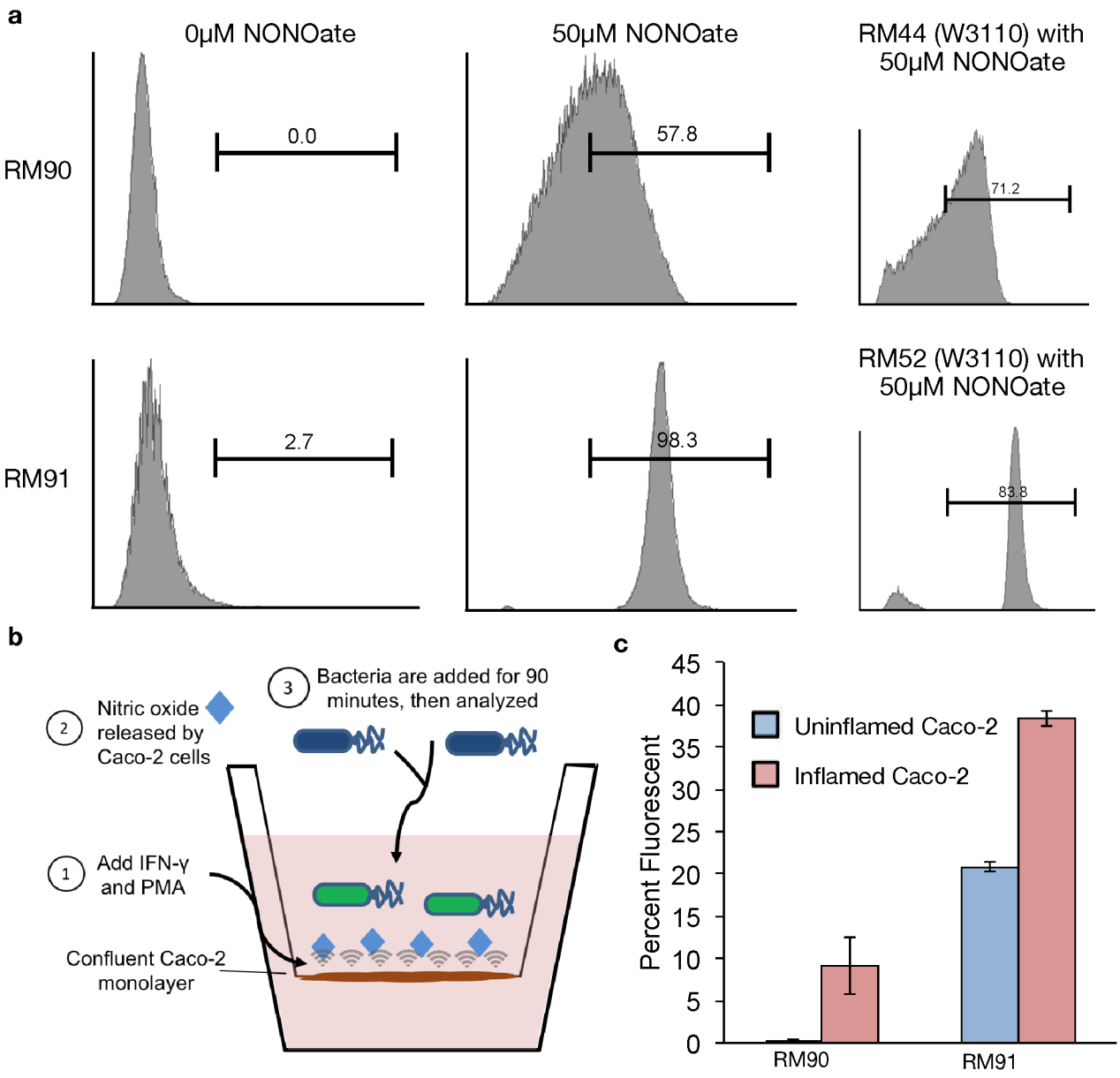

Figure 3. (a) Representative flow cytometry data of approximately 50,000 Nissle 1917 host cells per plot, using a FITC voltage of 400V after 90 minutes of induction. The gate to determine the fluorescent population is defined as anything above the population of a negative control of non-fluorescent cells. Y-axis is cell count and X-axis is FITC (fluorescence) intensity. **(b)** Schematic of the IBD *in vitro* assay to stimulate engineered bacteria with biologically produced NO. Bacteria are incubated in the apical side of the transwell insert and assessed via FACS. **(c)** The percentage of the total population of cells that are above a threshold fluorescence from the assay illustrated in (b), plot as the average of biological duplicates. Error bars are standard error.